Research Article
doi.org/10.1002/cmdc.202200382
Chemistry Europe
European Chemical Societies Publishing

www.chemmedchem.org

Toward a Home Test for COVID-19 Diagnosis: DNA Machine for Amplification-Free SARS-CoV-2 Detection in Clinical Samples

Ahmed A. El-Deeb,[a] Sofia S. Zablotskaya,[a] Maria S. Rubel,[a] Moustapha A. Y. Nour,[a] Liubov I. Kozlovskaya,[b] Anna A. Shtro,[c] Andrey B. Komissarov,[c] and Dmitry M. Kolpashchikov*[a, d, e]

Nucleic acid-based detection of RNA viruses requires an annealing procedure to obtain RNA/probe or RNA/primer complexes for unwinding stable structures of folded viral RNA. In this study, we designed a protein-enzyme-free nanoconstruction, named four-armed DNA machine (4DNM), that requires neither an amplification stage nor a high-temperature annealing step for SARS-CoV-2 detection. It uses a binary deoxyribozyme (BiDz) sensor incorporated in a DNA nanostructure equipped with a total of four RNA-binding arms. Additional arms were found to improve the limit of detection at least 10-fold. The sensor distinguished SARS-CoV-2 from other respiratory viruses and correctly identified five positive and six negative clinical samples verified by quantitative polymerase chain reaction (RT-qPCR). The strategy reported here can be used for the detection of long natural RNA and can become a basis for a point-of-care or home diagnostic test.

Introduction

Current testing capacity of respiratory infections cannot meet the unprecedented global demands for rapid, reliable, and accessible nucleic acid-based diagnostics.[1–3] Reveres transcription quantitative polymerase chain reaction (RT-PCR) is one of the most common techniques used for the diagnosis of severe acute respiratory syndrome coronavirus 2 (CoV2) infection. Several days of the wait time for the test results during ongoing CoV2 outbreak revealed imperfection of the RT-qPCR and calls for new inexpensive, accessible diagnostics affordable by general population outside the specialized laboratories.[1] Towards this goal, several RT-PCR-free CoV2 nucleic acid tests are under development including those based on loop-mediated isothermal amplification (LAMP),[4] recombinase polymerase amplification (RPA),[5] and nucleic acid base amplification (NASBA)[6] among others.[7] Majority of the tests, however, depend on nucleic acid amplification procedures, which require expensive reagents including perishable protein enzymes. The amplification step can also add false positive results due to sample degradation or contamination.[8] Amplification-free diagnostics would avoid the need to use instruments that require specialized laboratories and/or qualified personnel.[9] Visual[10] or tactile[11] signal outputs could be the most user-friendly as they would not require equipment. However, such assays have high limits of detection (LOD) and thus doomed to be dependent on nucleic acid amplification.[10e,d] We turned our attention to fluorescent binary RNA-cleaving deoxyribozyme (BiDz) probe.[12] BiDz can reach LOD down to 1–10 pM,[13] which is, to the best of our knowledge, the lowest among protein enzyme-free testing systems that do not use amplification cascades.[14] BiDz consists of two DNA strands, Dz_a and Dz_b in Figure 1A which hybridize to the analyzed nucleic acid and form Dz catalytic core followed by the cleavage of fluorophore and a quencher-labelled reporter substrate (F sub in Figure 1).[12] One advantage of BiDz is its ability to amplify the signal due to cleaving multiple F sub molecules. Another advantage is its high selectivity towards single nucleotide substitutions (SNS).[12,15] This is achieved by shortening Arm 2 complementary to the SNS site (Figure 1A). Short arm binds only the fully complementary, but not single base mismatched sequences.[15]

Results

Initially, optimization of the BiDz assay was performed using a synthetic DNA analyte containing the sequence of 15398–15487 of CoV2 RdRp gene (CoV2-DNA1 in Table S1 and Figure S1). It was

[a] A. A. El-Deeb, S. S. Zablotskaya, M. S. Rubel, M. A. Y. Nour, Prof. D. M. Kolpashchikov
Laboratory of Molecular Robotics and Biosensor Materials
SCAMT Institute, ITMO University
191002 Saint Petersburg (Russia)
E-mail: dmitry.kolpashchikov@ucf.edu
[b] Dr. L. I. Kozlovskaya
Chumakov Federal Scientific Center for Research and Development of Immune-and-Biological Products
Russian Academy of Sciences
Institute of Poliomyelitis, Moscow (Russia)
[c] Dr. A. A. Shtro, Dr. A. B. Komissarov
Smorodintsev Research Institute of Influenza
197376 Saint Petersburg (Russia)
[d] Prof. D. M. Kolpashchikov
Chemistry Department
University of Central Florida
Orlando, FL 32816 (USA)
[e] Prof. D. M. Kolpashchikov
Burnett School of Biomedical Sciences
University of Central Florida
Orlando, FL 32827 (USA)

Supporting information for this article is available on the WWW under https://doi.org/10.1002/cmdc.202200382

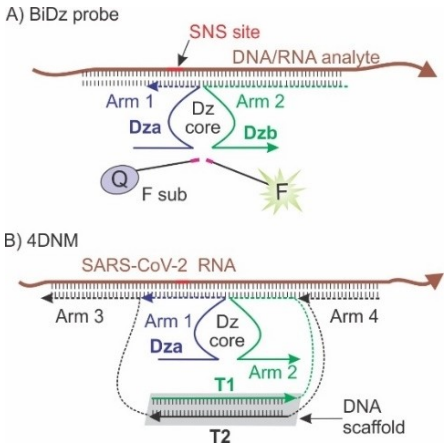

Figure 1. Design of the DNA constructs used in this study. A) BiDz probe: DNA strands Dz_a and Dz_b, bind RNA analyte and form the catalytic core that cleaves fluorophore and quencher labelled F sub. B) The four-armed DNA nanomachine (4DNM) has Dz_a and Dz_b attached to a double stranded DNA scaffold (shaded grey). Arms 3 and 4 are designed to tightly bind natural RNA, thereby unwinding its secondary structure. F sub is not shown.

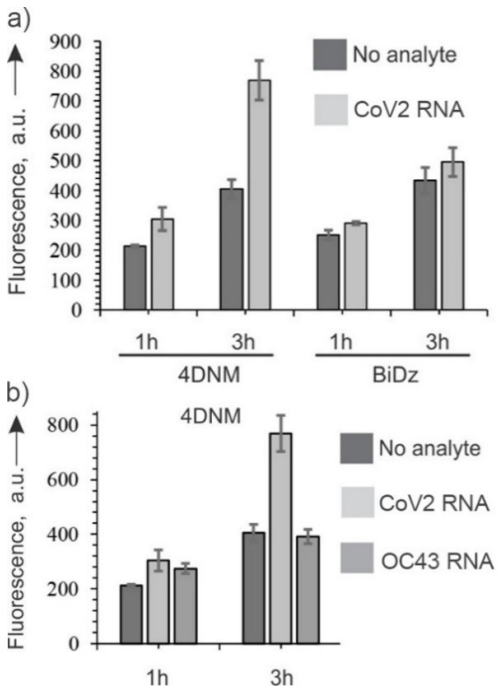

Figure 2. 4DNM selectively detects CoV2 RNA. A) Comparison of fluorescent response of 4DNM with BiDz in the absence or presence (dark grey and light grey bars, respectively) of 125 pM CoV2 RNA. F-sub (200 nM) was incubated with either BiDz (20 nM Dz_a and 5 nM Dz_b) or DNM (20 nM Dz_a and 5 nM of T1/T2 complex) in the presence 3.8×10^9 of either CoV2 or OC43 RNA molecules in a reaction buffer 1 (50 mM HEPES, pH 7.5, 150 mM KCl, 15 mM NaCl, 200 mM $MgCl_2$). Fluorescence at 517 nm ($\lambda_{ex}=485$ nm) was registered after 1 or 3 h of incubation at 55 °C. The error bars represent one standard deviation from average values calculated after three independent experiments. B) Selectivity of 4DNM machine. Fluorescent response of 4DNM to 3.8×10^9 molecules in 50 μL (125 pM) of CoV2 or OC43 RNA (See experimental section). The conditions were as described for panel A.

shown earlier that RdRp mutations are associated with CoV-2 genome evolution.[16] The BiDz probe was characterized by the LOD of 10 pM using the synthetic DNA analyte (Figure S3). This LOD is within the range of that reported earlier for the 10–23 BiDz.[12,13] However, when we used 125 pM CoV2 RNA extracted from the infected cells, we did not observe a signal significantly above the background (Figure 2). We hypothesized that viral RNA was folded in a stable secondary structure, which impeded probe binding and signal generation. This could be the reason why BiDz approach has not succeeded so far in clinically significant diagnostic formats.

To enable detection of long folded RNA, we designed a DNA nano-construction, named here 4DNM, equipped with two additional RNA binding arms, Arms 3 and 4 (Figure 1B). Arms 1, 3 and 4 attached to a dsDNA scaffold were designed to bind tightly to unwind the naturally folded viral RNA. Arm 2 was detached from the tile for a high recognition selectivity.[17] 4DNM produced signal ~2 times above the background when incubated with 125 pM CoV2 RNA (Figure 2A). Next, we tested selectivity of 4DNM. OC43 strain is known to be commonly associated with human infections.[18] It is important to differentiate CoV-2 from OC43 (as well as other strains) during clinical testing procedure. 4DNM reliably differentiated CoV2 from OC43 RNA samples isolated from infected cell culture (Figure 2B). CoV-2 -specific 4DNM differentiated also respiratory syncytial virus (RSV), Influenza virus A/PR/8/34 or parainfluenza HPIV-3 (Figure S4). This perfect selectivity is not surprising considering significant difference in the genomes of the alternative viruses and the ability of BiDz to differentiate single nucleotide substitutions in broad temperature ranges.[15]

We then investigated the ability of 4DNM to accurately recognize the presence of CoV2 in human clinical samples. RNA samples were isolated from 14 patients according to the standard procedure for RNA preparation for RT-qPCR.[18] Five samples were identified as negative, while nine as CoV2 positive. The cycle threshold (Ct) for the nine positive samples varied from 20.4 to 27.7 (see Figure 3 legend). All five negative samples 4DNM produced signals at the background level (samples 1–5, Figure 3). All but one positive sample with Ct 20.4 to 24.2 produced signal 40–50% above the background. While all samples with Ct 25.5-27.7 produced signal at the background level. This data indicates that sensitivity of 4DNM might be sufficient for detection of the samples with high but not with low viral load. Further investigations are required to establish clinical sensitivity and selectivity of the proposed detection technology as well as to identify the sources of the false signal obtained in this study.

Discussion

Long natural RNAs are folded in stable secondary structures, which are difficult to access for traditional hybridization probes. Amplification of such RNA samples require annealing step requiring heating equipment, which adds to the complexity and the cost of RNA analysis. BiDz probe was reported to be efficient in detecting short DNA analytes,[12–15] but is less successful in reporting the presence of long viral RNA as was found in this study (Figure 2A). Here, we proposed and tested the strategy for

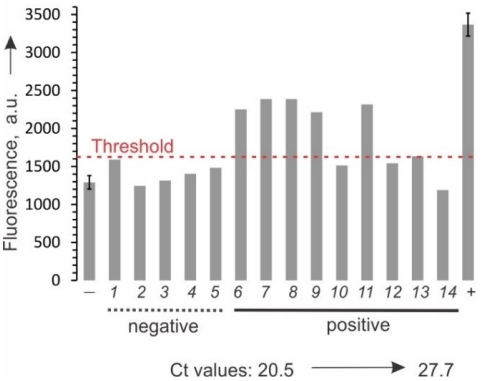

Figure 3. Analysis of clinical samples using 4DNM. All samples contained F-sub (200 nM) and 4DNM (20 nM Dza and 5 nM of T1/T2 complex) in reaction buffer 1 in the absence (−) or presence of clinical samples. Positive control (last bar) contained 20 pM of the synthetic CoV2-DNA1 analyte. Fluorescence at 517 nm (λ_{ex} = 485 nm) was registered after 3 h of incubation at 55 °C. Nine CoV-2 positive and five negative samples were collected from 14 different individuals and confirmed by RT-qPCR with indicated threshold cycle (Ct) values. The Ct values for positive samples were as follows: 6–20.4; 7–21.0; 8–21.8, 9–22.0; 10–22.9; 11–24.2; 12–25.5; 13–25.9; 14–27.7. Clinical samples 1–14 lack standard deviation since all available RNA from each sample was fully used only in one measurement to ensure the highest available concentration of viral RNA. Standard deviation for the negative (−) and the positive (+) controls were determined after three independent measurements. The threshold, line corresponds to 3 standard deviations above average (−) control.

designing a sensor that can efficiently recognize natural viral RNA. We took advantage of BiDz high sensitivity and equipped it with additional RNA-binding arms: Arm 3 and 4. As expected, this modification alone reduced LOD by at least 10 times and enabled detection of viral RNA isolated either from virus infected cell culture or patient samples with high viral load. Even though we did not attempt to investigate direct dynamic interaction between Arm 3 and 4, we hypothesized that improved LOD is the result of unfolding the RNA secondary structure powered by the thermodynamically favorable RNA/4DNM complex formation. Furthermore, Arm 3 and 4 as well as Dz_b strand were attached to the dsDNA platform via flexible hexaethylene glycol linkers (Table 1, Figure S1). This flexible connection might be important for accommodating catalytically active Dz core in proximity to bulky analyte and the dsDNA scaffold. The influence of linker flexibility on sensor performance should be further investigated. The strategy reported here can be adopted in the context of other probes for binding nucleic acids having stable secondary structures to avoid the annealing procedure and to achieve high yields of stable RNA-probe complex.

Amplification-free CoV2 tests were reported earlier.[9] For example, Shinoda et al. developed CRISPR/Cas13a targeting CoV2 genomic RNA.[9b] The system could reliably identify 5 negative and 5 positive clinical samples in a 2 h assay without any reported miss-identified samples. However, the system required tedious and expensive optimization of the three CRISPR/Cas13a complexes for targeting 3 different binding sites in CoV2 genome. CRISPR/Cas13a system relies on perishable protein enzymes and, therefore, will required low temperature storage facility. In this study, we developed an alternative amplification-free assay for detecting CoV2. The test does not require protein enzyme (e.g. Cas13a) and, therefore, promises to be less expensive and deliverable to the point-of-care settings without a need for refrigeration. Moreover, unlike CRISPR-based detection systems that take advantage of the non-sequence specific collateral RNA cleaving activity of CAS proteins, 4DNM can be adopted for multiplex assays.[19] Another 4DNM advantage over CRISPR/Cas-based test systems is the lack of requirement for protospacer adjacent motif to be present in the analyzed sequence, which limits the choice of the target sequences for cas-based systems.[20] 4DNM identified positive and negative samples accurately with a single false negative result for samples with high viral LOD (samples 6–11 in Figure 3). The source of this false negative could be the RNA degradation during storage and transportation, which could be avoided if the testing is done in short time after sample collection.

One possible limitation of 4DNM assay is its LOD, which is higher than that of RT-qPCR capable of detecting 10 viral particles.[1] However, modeling of viral dynamics suggests that LOD of 100,000 viral particles/mL (0.1 fM) is sufficient for screening and that frequent testing with a fast turnaround time rather than low LOD is required to break a pandemic.[21] LOD of 10^6 viral particle/mL (0.1 pM) is sufficient for this purpose as samples with the lower load are less infectious.[21] 4DNM responded with roughly the same intensity for the samples with different Ct (compare sample 6 and 11 with Ct difference of ~4). This observation requires further investigation since in this work 4NDM and Ct measurements were done at different time and locations, thus samples transportation and storage could affect

Table 1. Oligonucleotides used in this study.[a]

Name	Sequence 5′→3′	Purification
F-sub	AAG GTT(F) TCC TCg uCCC TGG GCA-BHQ1	HPLC
COV2-DNA1	ATT AGC TAA TGA GTG TGC TCA AGT ATT GAG TGA AAT GGT CAT GTG TGG CGG TTC ACT ATA TGT TAA ACC AGG TGG AAC CTC ATC AGG AG	SD
Dza	TGC CCA GG G **AG GCT AGC T** CA CAT GAC CAT TTC ACT CAA T	SD
Dzb	AAC ATA TAG TGA ACC GCC **AAC GA** G AGG AAA CCT T	SD
T1	ATC ACA TAC ACT ATG AGA CTA TGC GTA ACA TGC CTC TG TTA ACT TA/HEG/AAC ATA TAG TGA ACC GCC A**AC GA**G AGG AAA CCT T	HPLC
T2	ATG AGG TTC CAC CTG GTT/HEG/TAA GTT AAC AGA GGC ATG TTAC GCA TAG TCT CAT AGT GTA TGT GAT/HEG/CTT GAG CAC ACT CAT TAG CTA AT	HPLC

[a] RNA nucleotides are in lower case; nucleotides in bold are the Dz 10–23 catalytic core; underlined nucleotides are F-sub binding arms. (F): fluorescein; BHQ1: black hole quencher 1; HPLC: high-pressure liquid chromatography; SD: Standard desalting; HEG: hexaethylene glycol.

the quality of RNA samples. Further LOD improvements and assay shortening can include the following strategies: sample concentration, using multiple 4DNM for binding the same RNA molecule[13] or adopting the DNA antenna tile design for facilitated substrate delivery to the activated Dz core.[17] 4DNM proposed here can become an advantageous tool for detection of SNS in clinically significant DNA or RNA, for example in identification of bacterial resistance to antibiotics. Indeed, unlike less selective CRISPR/Cas systems,[20] BiDz sensors can easily differentiate SNS under broadly variable experimental conditions.[15]

Conclusion

In conclusion, we have demonstrated that the multi-armed strategy enables amplification-free detection of viral RNA. The strategy eliminates the need for probe/target annealing step otherwise required by all know methods for RNA detection. The detection system is a good starting point for the development of low-cost point of care or home test for CoV2 or other infections.

Experimental Section

4DNM assembly. T1 and T2, (Table 1) were mixed in 100 nM concentration in Reaction buffer 1 (50 mM $MgCl_2$, 50 mM HEPES, pH 7.4, 150 mM KCl, 15 mM NaCl). The sample was incubated in a boiling water bath followed by overnight cooling to room temperature. The accuracy of association was tested by native polyacrylamide gel electrophoresis (PAGE) as shown in Figure S2.

Cell culture and clinical material handling. SARS-CoV-2 particles were harvested from Vero cell line as described earlier.[22] The virus was added to the 24 h culture of Vero cell confluent monolayers and incubated for 1 h at room temperature. The virus titer was 6.7× logTCID50/100μL. Culture medium containing antibiotics and 16 μg/mL trypsin was then added. The cells were incubated at 37 °C and observed daily for signs of a cytopathic effect. On the 6th day after infection, cell culture suspensions were collected and viral particles were extracted with the RNAeasy Kit, Qiagen. Presence of viral RNA was examined by the RT-PCR quantification kit (POLYVIR SARS-CoV-2, Lytech, Russia).

HCoV-OC43 particles were obtained from a strain presented by Gamaleya Institute, Moscow, Russia. Confluent Vero 81 cells were infected with inoculating suspension after 1 day of growth at 37 °C, 90% humidity, 5% CO_2. Cells and virus were incubated together for 1 h and then 2 μg/mL of Ciprofloxacin and 1 μg/mL of trypsin were added. The cytopathic effect was confirmed after 21 h infection followed by RNA extraction via a standard phenol-chloroform protocol.

Influenza virus A/PR/8/34 was grown in chicken embryo as described earlier.[23] RSV PCB A2 strain was grown in as described earlier[24] Parainfluenza HPIV-3 was grown on HEp2 cell line as described earlier.[25]

Calculation of viral RNA concentration in genome equivalents (G.E.). Number G.E. of viral RNA was calculated as follows: copy number per microliter (CN) = C (RNA) $g\times\mu L^{-1}$/m (1 viral RNA genome); $CN = 12.68\times10^{-9}\ g\times\mu L^{-1}/1.59\times10^{-17}\ g \approx 8\times10^{8}\ \mu L^{-1}$. In 4.75 μL sample used for each sample $CN = 8\times10^{8}\ \mu L^{-1\times}4.75\ \mu L = 3.8\times10^{9}$ G.E. Conversion of G.E. to molar concentration was as follows: $(3.8\times10^{9}\ G.E./6.02\times10^{23}\times mol^{-1})/50\ \mu L = 1.25\times10^{-10}$ M or 125 pM.

Clinical samples. Clinical samples were collected as nasopharyngeal swabs among patients of hospital with RT-PCR confirmed CoV-2. RNA of the clinical samples was extracted via the RNAeasy Kit (Qiagen). The presence of Cov-2 was confirmed with HKU protocol.[26] Samples with Ct in the range of 16–27 were used.

Fluorescent assay. A conservative region of the RdRp gene was chosen for probing.[27] Statistics were carried out according to analytical guidelines. The samples were incubated in Reaction Buffer 1 at 55°C for 1 and 3 h in water bath. After incubation, the samples were cooled to room temperature followed by fluorescent measurement $\lambda_{Ex}/\lambda_{Em} = 480/525$ nm.

Samples of viral particles or synthetic DNA were incubated in Col buffer (final concentration: 200 mM $MgCl_2$, 200 mM HEPES, pH 7.4, 150 mM KCl, 15 mM NaCl) in a presence of 200 nM F-sub (reporting molecule, Supporting Information Table S1), 20 nM of the separated arm (Dzb, Table S1), and 5 nM of the annealed 4DNM (T1/T2 complex) in the absence or presence of various concentrations of synthetic analyte ranging from 20 pM to 0.1 pM. The samples were incubated for 1 or 3 h at 55 °C in water bath and the resulted fluorescence was detected using Spark fluorescent plate reader (Tecan, Switzerland). Limit-of-detection was calculated according to the earlier established guidelines.[28]

Supporting Information

The Supporting Information contains details 4DNM design and assembly, and data for LOD measurement.

Author Contributions

A.A.E. was responsible for experimental design, acquisition of experimental data, data analysis and manuscript preparation; S.S.Z and M.A.Y.N. data acquisition and analysis; M.S.R. handled project administration, data analysis and manuscript preparation; L.I.K., A.A.S., and A.B.K. provided resources, discussed results, edited the manuscript, D.M.K. designed research, analyzed data, and contributed to manuscript preparation. The manuscript was written through contributions of all authors. All authors have given approval to the final version of the manuscript.

Acknowledgements

The study was supported by the Russian Science Foundation N° 22-24-00664 to Daria D. Nedorezova and by SCAMT Institute, ITMO University, Saint-Petersburg, Russia. The authors are grateful to Olga Gancharova for donation of the viral RNA.

Conflict of Interest

The authors declare no conflict of interest.

Data Availability Statement

Research data are not shared.

Keywords: detection of folded RNA · 10-23 DNAzyme · deoxyribozyme sensor · binary hybridization probe · DNA machine

[1] W. Feng, A. M. Newbigging, C. Le, B. Pang, H. Peng, Y. Cao, J. Wu, G. Abbas, J. Song, D. B. Wang, M. Cui, J. Tao, D. L. Tyrrell, X. E. Zhang, H. Zhang, X. C. Le, *Anal. Chem.* **2020**, *92*, 10196–10209.

[2] a) P. Pokhrel, C. Hu, H. Mao, *ACS Sens.* **2020**, *5*, 2283–2296; b) D. K. Nurputra, A. Kusumaatmaja, M. S. Hakim, S. N. Hidayat, T. Julian, B. Sumanto, Y. Mahendradhata, A. M. I. Saktiawati, H. S. Wasisto, K. Triyana, *NPJ Digit. Med.* **2022**, *5*, 115, https://pubmed.ncbi.nlm.nih.gov/35974062/; c) A. S. Ignaszak, *Adv. Mater. Technol.* **2022**, 2200208, https://pubmed.ncbi.nlm.nih.gov/35942251/; d) A. N. Masterson, R. Sardar, *ACS Appl. Mater. Interfaces* **2022**, Online ahead of print acsami.2c06599, https://pubmed.ncbi.nlm.nih.gov/35639080/; e) M. Borro, G. Salerno, A. Montori, A. Petrucca, P. Anibaldi, A. Marcolongo, R. Bonfini, M. Simmaco, I. Santino, *Healthcare* **2022**, *10*, 790, https://pubmed.ncbi.nlm.nih.gov/35627926/; f) L. T. Nguyen, S. R. Rananaware, B. L. M. Pizzano, B. T. Stone, P. K. Jain, *Commun Med (Lond).* **2022**, *2*, 7, https://pubmed.ncbi.nlm.nih.gov/35603267/.

[3] a) I. A. Mattioli, A. Hassan, O. N. Oliveira, F. N. Crespilho, *ACS Sens.* **2020**, *5*, 3655–3677, https://pubmed.ncbi.nlm.nih.gov/33267587/; b) S. J. R. da Silva, J. C. F. do Nascimento, R. P. Germano Mendes, K. M. Guarines, C. Targino Alves da Silva, P. G. da Silva, J. J. F. de Magalhães, J. R. J. Vigar, A. Silva-Júnior, A. Kohl, K. Pardee, L. Pena, *ACS Infect. Dis.* **2022**, *8*, 758–1814; c) S. Tazi, H. Kabbaj, J. Zirar, A. Zouaki, G. El Amin, O. El Himeur, M. Seffar, *Adv. Virol.* **2022**, *2022*, 4510900, https://pubmed.ncbi.nlm.nih.gov/35693128/; d) M. Jiang, T. Dong, C. Han, L. Liu, T. Zhang, Q. Kang, P. Wang, F. Zhou, *Anal. Chim. Acta* **2022**, *1208*, 339830.

[4] a) O. E. Anastasiou, C. Holtkamp, M. Schäfer, F. Schön, A. M. Eis-Hübinger, A. Krumbholz, *Viruses* **2021**, *13*, 801; b) A. Ganguli, A. Mostafa, J. Berger, J. Lim, E. Araud, J. Baek, S. A. Stewart de Ramirez, A. Baltaji, K. Roth, M. Aamir, S. Aedma, M. Mady, P. Mahajan, S. Sathe, M. Johnson, K. White, J. Kumar, E. Valera, R. Bashir, *Anal. Chem.* **2021**, *93*, 7797–7807; c) Y. He, T. Xie, Y. Tong, *Biosens. Bioelectron.* **2021**, *187*, 113330; d) S. Sherrill-Mix, Y. Hwang, A. M. Roche, A. Glascock, S. R. Weiss, Y. Li, L. Haddad, P. Deraska, C. Monahan, A. Kromer, J. Graham-Wooten, L. J. Taylor, B. S. Abella, A. Ganguly, R. G. Collman, G. D. Van Duyne, F. D. Bushman, *Genome Biol.* **2021**, *22*, 169.

[5] a) D. Cherkaoui, D. Huang, B. S. Miller, V. Turbé, R. A. McKendry, *Biosens. Bioelectron.* **2021**, *189*, 113328; b) H. E. Kim, A. Schuck, S. H. Lee, Y. Lee, M. Kang, Y.-S. Kim, *Biosens. Bioelectron.* **2021**, *182*, 113168; c) W. S. Zhang, J. Pan, F. Li, M. Zhu, M. Xu, H. Zhu, Y. Yu, G. Su, *Anal. Chem.* **2021**, *93*, 4126–4133.

[6] M. C. Keightley, P. Sillekens, W. Schippers, C. Rinaldo, K. S. George, *J. Med. Virol.* **2005**, *77*, 602–608.

[7] a) Q. Wu, C. Suo, T. Brown, T. Wang, S. A. Teichmann, A. R. Bassett, *Sci. Adv.* **2021**, *7*, eabe5054; b) K. R. Alkharsah, *Ger. Med.* **2021**, *19*, 1–12; c) G. Aquino-Jarquin, *Drug Discov Today* **2021**, *26*, 2025–2035, https://pubmed.ncbi.nlm.nih.gov/34147688/; d) J. P. Broughton, X. Deng, G. Yu, C. L. Fasching, V. Servellita, J. Singh, X. Miao, J. A. Streithorst, A. Granados, A. Sotomayor-Gonzalez, K. Zorn, A. Gopez, E. Hsu, W. Gu, S. Miller, C.-Y. Pan, H. Guevara, D. A. Wadford, J. S. Chen, C. Y. Chiu, *Nat. Biotechnol.* **2020**, *38*, 870–874; e) S. Kelley, *ACS Sens.* **2021**, *6*, 1407.

[8] R. Rahbari, N. Moradi, M. Abdi, *Clin. Chim. Acta.* **2021**, *516*, 1–7.

[9] a) P. Fozouni, S. Son, M. Díaz de León Derby, G. J. Knott, C. N. Gray, M. V. D'Ambrosio, C. Zhao, N. A. Switz, G. R. Kumar, S. I. Stephens, D. Boehm, C.-L. Tsou, J. Shu, A. Bhuiya, M. Armstrong, A. R. Harris, P.-Y. Chen, J. M. Osterloh, A. Meyer-Franke, B. Joehnk, K. Walcott, A. Sil, C. Langelier, K. S. Pollard, E. D. Crawford, A. S. Puschnik, M. Phelps, A. Kistler, J. L. DeRisi, J. A. Doudna, D. A. Fletcher, M. Ott, *Cell* **2021**, *184*, 323–333; b) L. Kashefi-Kheyrabadi, H. V. Nguyen, A. Go, C. Baek, N. Jang, J. M. Lee, N.-H. Cho, J. Min, M.-H. Lee, *Biosens. Bioelectron.* **2021**, *195*, 113649; c) H. Shinoda, Y. Taguchi, R. Nakagawa, A. Makino, S. Okazaki, M. Nakano, Y. Muramoto, C. Takahashi, I. Takahashi, J. Ando, T. Noda, O. Nureki, H. Nishimasu, R. Watanabe, *Commun. Biol.* **2021**, *4*, 476.

[10] a) D. M. Kolpashchikov, *Am. Chem.* **2008**, *130*, 2934–2935; b) Y. V. Gerasimova, E. M. Cornett, E. Edwards, X. Su, K. H. Rohde, D. M. Kolpashchikov, *ChemBioChem* **2013**, *14*, 2087–2090; c) B. C. Dhar, A. J. Reed, S. Mitra, P. Rodriguez Sanchez, D. D. Nedorezova, R. P. Connelly, K. H. Rohde, Y. V. Gerasimova, *Biosens. Bioelectron.* **2020**, *165*, 112385; d) E. A. Kovtunov, L. A. Shkodenko, E. A. Goncharova, D. D. Nedorezova, S. V. Sidorenko, E. I. Koshel, D. M. Kolpashchikov, *ChemistrySelect* **2020**, *5*, 14572–14577; e) D. A. Gorbenko, L. A. Shkodenko, M. S. Rubel, A. V. Slita, E. V. Nikitina, E. A. Martens, D. Kolpashchikov, *Chem. Commun.* **2022**, *58*, 5395–5398.

[11] a) T. A. Fedotova, D. M. Kolpashchikov, *Chem. Commun.* **2017**, *53*, 12622–12625; b) Y. V. Lanchuk, S. A. Ulasevich, T. A. Fedotova, D. M. Kolpashchikov, E. V. Skorb, *RSC Adv.* **2018**, *66*, 37735–37739.

[12] a) D. M. Kolpashchikov, *ChemBioChem* **2007**, *8*, 2039–2042; b) E. Mokany, S. M. Bone, P. E. Young, T. B. Doan, A. V. Todd, *J. Am. Chem. Soc.* **2010**, *132*, 1051–1059; c) Y. V. Gerasimova, A. Hayson, J. Ballantyne, D. M. Kolpashchikov, *ChemBioChem* **2010**, *11*, 1762–1768; d) Y. V. Gerasimova, D. M. Kolpashchikov, *Chem. Biol.* **2010**, *17*, 104–106.

[13] Y. V. Gerasimova, D. M. Kolpashchikov, *Angew. Chem. Int. Ed. Engl.* **2013**, *52*, 10586–10588.

[14] N. Hasick, A. Lawrence, R. Ramadas, A. Todd, *Molecules* **2020**, *25*, 1755.

[15] a) A. J. Reed, R. J. Sapia, C. Dowis, S. Solarez, Y. V. Gerasimova, *RNA.* **2020**, *26*, 1882–1890; b) A. L. Smith, D. M. Kolpashchikov, *ChemistrySelect* **2017**, *2*, 5427–5431; c) J. Grimes, Y. V. Gerasimova, D. M. Kolpashchikov, *Angew. Chem. Int. Ed. Engl.* **2010**, *49*, 8950–8953.

[16] V. M. Corman, O. Landt, M. Kaiser, R. Molenkamp, A. Meijer, D. K. Chu, T. Bleicker, S. Brünink, J. Schneider, M. L. Schmidt, D. G. Mulders, B. L. Haagmans, B. van der Veer, S. van den Brink, L. Wijsman, G. Goderski, J.-L. Romette, J. Ellis, M. Zambon, M. Peiris, H. Goossens, C. Reusken, M. P. Koopmans, C. Drosten, *Euro Surveill* **2020**, *25*, 2000045, https://pubmed.ncbi.nlm.nih.gov/31992387/.

[17] a) A. J. Cox, H. N. Bengtson, Y. V. Gerasimova, K. H. Rohde, D. M. Kolpashchikov, *ChemBioChem* **2016**, *17*, 2038–2041; b) A. J. Cox, H. N. Bengtson, K. H. Rohde, D. M. Kolpashchikov, *Chem. Commun.* **2016**, *52*, 14318–14321.

[18] A. Komissarov, A. Fadeev, A. Kosheleva, K. Sintsova, M. Grudinin, *Mol. Cell. Probes* **2017**, *35*, 57–63.

[19] E. Mokany, A. V. Todd, *Methods Mol. Biol.* **2013**, *1039*, 31–49.

[20] M. Klein, B. slami-Mossallam, D. G. Arroyo, M. Depken, *Cell Rep.* **2018**, *22*, 1413–1423.

[21] D. B. Larremore, B. Wilder, E. Lester, S. Shehata, J. M. Burke, J. A. Hay, M. Tambe, M. J. Mina, R. Parker, *Sci. Adv.* **2021**, *7*, eabd5393.

[22] L. Kozlovskaya, A. Piniaeva, G. Ignatyev, A. Selivanov, A. Shishova, A. Kovpak, I. Gordeychuk, Y. Ivin, A. Berestovskaya, E. Prokhortchouk, D. Protsenko, M. Rychev, A. Ishmukhametov, *Int. J. Infect. Dis.* **2020**, *99*, 40–46, https://pubmed.ncbi.nlm.nih.gov/32721529/.

[23] A. S. Sokolova, O. I. Yarovaya, D. V. Baranova, A. V. Galochkina, A. A. Shtro, M. V. Kireeva, S. S. Borisevich, Y. V. Gatilov, V. V. Zarubaev, N. F. Salakhutdinov, *Arch. Virol.* **2021**, *166*, 1965–1976.

[24] T. M. Khomenko, A. A. Shtro, A. V. Galochkina, Y. V. Nikolaeva, G. D. Petukhova, S. S. Borisevich, D. V. Korchagina, K. P. Volcho, N. F. Salakhutdinov, *Molecules* **2021**, *26*, 7493.

[25] A. P. Durbin, S. L. Hall, J. W. Siew, S. S. Whitehead, P. L. Collins, B. R. Murphy, *Virology* **1997**, *235*, 323–332.

[26] D. K. W. Chu, Y. Pan, S. M. S. Cheng, K. P. Y. Hui, P. Krishnan, Y. Liu, D. Y. M. Ng, C. K. C. Wan, P. Yang, Q. Wang, M. Peiris, L. L. M. Poon, *Clin. Chem.* **2020**, *66*, 549–555.

[27] V. M. Corman, O. Landt, M. Kaiser, R. Molenkamp, A. Meijer, D. K. Chu, T. Bleicker, S. Brünink, J. Schneider, M. L. Schmidt, D. G. Mulders, B. L. Haagmans, B. van der Veer, S. van den Brink, L. Wijsman, G. Goderski, J.-L. Romette, J. Ellis, M. Zambon, M. Peiris, H. Goossens, C. Reusken, M. P. Koopmans, C. Drosten, *Euro Surveill* **2020**, *25*, 2000045.

[28] G. L. Long, J. D. Winefordner, *Anal. Chem.* **1983**, *55*, 712 A–724 A.

Manuscript received: July 14, 2022
Revised manuscript received: August 26, 2022
Accepted manuscript online: August 28, 2022
Version of record online: ■■, ■■■

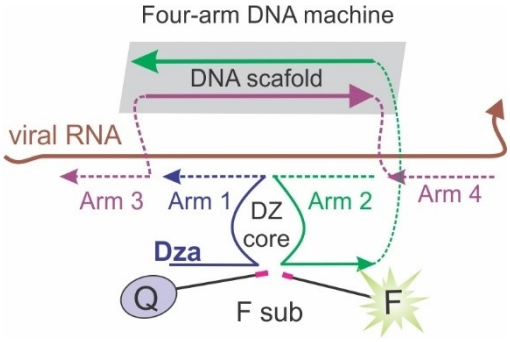

*A. A. El-Deeb, S. S. Zablotskaya, M. S. Rubel, M. A. Y. Nour, Dr. L. I. Kozlovskaya, Dr. A. A. Shtro, Dr. A. B. Komissarov, Prof. D. M. Kolpashchikov**

1 – 6

Toward a Home Test for COVID-19 Diagnosis: DNA Machine for Amplification-Free SARS-CoV-2 Detection in Clinical Samples

Nucleic acid-based detection of RNA viruses requires an annealing procedure to obtain RNA/probe or RNA/primer complexes for unwinding stable structures of folded viral RNA. We designed a protein-enzyme-free nano-construction, termed a four-armed DNA machine (4DNM), that requires neither an amplification stage nor a high-temperature annealing step for SARS-CoV-2 detection. This strategy can be used for detecting long natural RNA inpoint-of-care or home diagnostic tests.